U-Load Dextramer®
Build multimers with your choice of peptide and peptide-receptive MHC I and MHC II alleles.

The Journal of Immunology

Sphingosine 1-Phosphate–Induced Motility and Endocytosis of Dendritic Cells Is Regulated by SWAP-70 through RhoA

This information is current as of February 24, 2022.

Carlos Ocaña-Morgner, Peter Reichardt, Michaël Chopin, Sarah Braungart, Christine Wahren, Matthias Gunzer and Rolf Jessberger

J Immunol 2011; 186:5345-5355; Prepublished online 18 March 2011;
doi: 10.4049/jimmunol.1003461
http://www.jimmunol.org/content/186/9/5345

Supplementary Material http://www.jimmunol.org/content/suppl/2011/03/18/jimmunol.1003461.DC1

References This article **cites 55 articles**, 25 of which you can access for free at:
http://www.jimmunol.org/content/186/9/5345.full#ref-list-1

Why *The JI*? Submit online.

- **Rapid Reviews! 30 days*** from submission to initial decision
- **No Triage!** Every submission reviewed by practicing scientists
- **Fast Publication!** 4 weeks from acceptance to publication

**average*

Subscription Information about subscribing to *The Journal of Immunology* is online at:
http://jimmunol.org/subscription

Permissions Submit copyright permission requests at:
http://www.aai.org/About/Publications/JI/copyright.html

Email Alerts Receive free email-alerts when new articles cite this article. Sign up at:
http://jimmunol.org/alerts

The Journal of Immunology is published twice each month by
The American Association of Immunologists, Inc.,
1451 Rockville Pike, Suite 650, Rockville, MD 20852
Copyright © 2011 by The American Association of Immunologists, Inc. All rights reserved.
Print ISSN: 0022-1767 Online ISSN: 1550-6606.

Downloaded from http://www.jimmunol.org/ by guest on February 24, 2022

Sphingosine 1-Phosphate–Induced Motility and Endocytosis of Dendritic Cells Is Regulated by SWAP-70 through RhoA

Carlos Ocaña-Morgner,* Peter Reichardt,† Michaël Chopin,* Sarah Braungart,* Christine Wahren,* Matthias Gunzer,† and Rolf Jessberger*

The phospholipid mediator sphingosine 1-phosphate (S1P) enhances motility and endocytosis of mature dendritic cells (DCs). We show that in vitro migration of *Swap-70*$^{-/-}$ bone marrow-derived DCs (BMDCs) in response to S1P and S1P-induced upregulation of endocytosis are significantly reduced. S1P-stimulated movement of *Swap-70*$^{-/-}$ BMDCs, specifically retraction of their trailing edge, in a collagen three-dimensional environment is impaired. These in vitro observations correlate with delayed entry into lymphatic vessels and migration to lymph nodes of skin DCs in *Swap-70*$^{-/-}$ mice. Expression of S1P receptors ($S1P_{1-3}$) by wild-type and *Swap-70*$^{-/-}$ BMDCs is similar, but *Swap-70*$^{-/-}$ BMDCs fail to activate RhoA and to localize Rac1 and RhoA into areas of actin polymerization after S1P stimulus. The Rho-activating G protein $G\alpha_i$ interacts with SWAP-70, which also supports the localization of $G\alpha_{13}$ to membrane rafts in BMDCs. LPS-matured *Swap-70*$^{-/-}$ BMDCs contain significantly more active RhoA than wild-type DCs. Preinhibition of Rho activation restored migration to S1P, S1P-induced upregulation of endocytosis in mature *Swap-70*$^{-/-}$ BMDCs, and localization of $G\alpha_{13}$ to membrane rafts. These data demonstrate SWAP-70 as a novel regulator of S1P signaling necessary for DC motility and endocytosis. ***The Journal of Immunology*, 2011, 186: 5345–5355.**

Uptake of Ag by dendritic cells (DCs) and their subsequent maturation and movements to lymphoid tissue to present to and activate T lymphocytes are key to initiate an adaptive immune response (1). Elucidating the mechanisms that regulate DC motility and Ag uptake is important also to design vaccination strategies and treatment of infections.

Sphingosine 1-phosphate (S1P) acts as a chemoattractant in the blood and lymph at concentrations in the hundred-nanomolar range (2). S1P promotes lymphocyte egress from lymphoid organs (3) and, as revealed through studies using S1P agonists and S1P receptor knockout mice, regulates migration of mature DCs from skin or lung to draining lymph nodes in vivo (4–8). S1P signals through G protein-coupled receptors (GPCRs) named $S1P_{1-5}$. These receptors execute different cellular functions through coupling to distinct heterotrimeric G proteins (α_i, α_q, or $\alpha_{12/13}$), resulting in activation of the small Rho GTPase family members Rac, RhoA, and/or Cdc42. Diversity in the expression of S1P receptors and in the response to S1P is seen among several cell types. The regulation of cell motility is a main function of these receptors (9, 10). In mature DCs, motility toward S1P is modulated by $S1P_1$ and $S1P_3$ (4, 5, 8, 11, 12). The in vitro observation that S1P induces upregulation of endocytosis in matured DCs suggests that S1P may promote the rapid removal of bacteria at sites of infection (11). $S1P_1$ activates Rac1 after coupling $G\alpha_I$, whereas $S1P_3$ activates Rac1 and RhoA after association with $G\alpha_i$ and $G\alpha_{12/13}$, respectively (10). The importance of S1P to control motility and endocytosis of mature DCs has clearly been demonstrated, but regulatory mechanisms that govern the S1P signaling pathways in DCs remain to be fully understood.

SWAP-70 is expressed in DCs and localizes to DC membranes at sites of cell–cell contact and of micropinosomes (13). Functionally, SWAP-70 supports surface localization of peptide-loaded MHC class II (MHC-II) on DCs (14). Maturation of DCs triggers massive cytoskeletal rearrangements mainly controlled by activation of Rho GTPases (15, 16), which also regulate DC migration (16–20). SWAP-70 loosely resembles proteins of the Dbl family of guanine nucleotide exchange factors for Rho GTPases, and it binds to F-actin and Rac (21, 22). We demonstrated that SWAP-70 preferentially interacts with active RhoA (RhoA-GTP) and Rac1 (Rac1-GTP) in lysates of stimulated DCs. Unlike naive wild-type (wt) bone marrow-derived DCs (BMDCs), naive *Swap-70*$^{-/-}$ DCs show constitutively active RhoA (14). On LPS stimulation, further Rho activation fails in *Swap-70*$^{-/-}$ DCs. Considering the function of SWAP-70 to regulate Rho GTPases, we hypothesized that SWAP-70 affects S1P receptor signaling required for migration of DCs.

In this study, we aimed at testing this hypothesis. We demonstrate the requirement for SWAP-70 in RhoA-dependent, S1P-dependent motility and endocytosis of DCs. *Swap-70*$^{-/-}$ BMDCs show deficient upregulation of motility and endocytosis in response to S1P. Migration to S1P is restored by re-expression of SWAP-70 in *Swap-70*$^{-/-}$ BMDCs. Analysis of Rho GTPase activation in mature *Swap-70*$^{-/-}$ BMDCs revealed that *Swap-70*$^{-/-}$ BMDCs fail to activate RhoA after an S1P stimulus. In BMDCs lysates, SWAP-70 was shown to interact with the proteins $G\alpha_i$. *Swap-70*$^{-/-}$ BMDCs also fail to localize the signaling protein $G\alpha_{13}$ required for RhoA activation to membrane rafts. These results thus highlight a novel pathway of S1P-induced DC functions.

*Faculty of Medicine Carl Gustav Carus, Institute of Physiological Chemistry, Dresden University of Technology, D-01307 Dresden, Germany; and †Institute of Molecular and Clinical Immunology, Otto von Guericke University Magdeburg, 39120 Magdeburg, Germany

Received for publication October 19, 2010. Accepted for publication February 18, 2011.

Address correspondence and reprint requests to Prof. Carlos Ocaña-Morgner and Prof. Rolf Jessberger, Institute of Physiological Chemistry, Faculty of Medicine Carl Gustav Carus, Dresden University of Technology, Fiedlerstrasse 42, MTZ, Dresden 01307, Germany. E-mail addresses: carlos.ocana-morgner@mailbox.tu-dresden.de and rolf.jessberger@mailbox.tu-dresden.de

The online version of this article contains supplemental material.

Abbreviations used in this article: BMDC, bone marrow-derived dendritic cell; DC, dendritic cell; 2D, two-dimensional; 3D, three-dimensional; GPCR, G protein-coupled receptor; MHC class II, MHC-II; S1P, sphingosine 1-phosphate; wt, wild-type.

Copyright © 2011 by The American Association of Immunologists, Inc. 0022-1767/11/$16.00

www.jimmunol.org/cgi/doi/10.4049/jimmunol.1003461

Downloaded from http://www.jimmunol.org/ by guest on February 24, 2022

Materials and Methods

Animals

Swap-70$^{-/-}$ and the isogenic wt 129vEMS mice were described before (14) and maintained at the Experimental Center of the Medizinisch-Theoretisches Zentrum of the Medical Faculty at the Dresden University of Technology according to approved animal welfare guidelines.

BMDC cultures

Primary cultures of immature DCs from *Swap-70*$^{-/-}$ and wt 129vEMS mice were obtained by differentiation of bone marrow-derived precursors as described previously (14). At days 10–11, 1 μg/ml LPS (Sigma-Aldrich; *Salmonella enterica*) was added overnight. For most of the experiments, CD11c$^+$ BMDCs were then purified from cultures using anti-CD11c Abs bound to magnetic beads (Miltenyi Biotec). For activation of Rho GTPases, BMDCs were activated with LPS and then starved from GM-CSF for 4 h before S1P stimulus.

Real time-PCR

Total BMDC RNA was prepared using the TRIzol method (Invitrogen) according to the manufacturer's instructions. RNA was reverse transcribed (SuperScript reverse transcriptase; Invitrogen). Expression of S1P1, S1P2, S1P3, and GAPDH was analyzed using a Rotor-Gene RG3000 (Qiagen) and the DNA Master Plus SYBR Green Kit (Roche). The relative gene expression was calculated by dividing by the expression of GAPDH. Samples were amplified in duplicate. S1P1, S1P2, and S1P3 primers used were previously described (23): S1P1 forward, 5′-GTGTAGACCCAGAGTC-CTGCG-3′; S1P1 reverse, 5′-AGCTTTTCCTTGGCTGGAGAG-3′; S1P2 forward, 5′-GGCCTAGCCAGTGCTCAGC-3′; S1P2 reverse, 5′-CCTTG-GTGTAATTGTAGTGTTCCAGA-3′; S1P3 forward, 5′-GGAGCCCCTA-GACGGGAGT-3′; S1P3 reverse, 5′-CCGACTGCGGGAAGAGTGT-3′. PCR product sizes were as follows: S1P1, 88 bp; S1P2, 118 bp; S1P3, 104 bp.

Flow cytometry

LPS-stimulated BMDCs were used to detect the expression of receptors $S1P_1$ and $S1P_3$ on the surface of the cells using an LSRII flow cytometer and FACSDiva software (BD Biosciences). Polyclonal Abs against $S1P_1$ and $S1P_3$ were used at a concentration of 4 μg/ml (Cayman Chemical). FITC-labeled goat anti-rabbit IgG (SouthernBiotech) was used as secondary Ab at a dilution of 1:250.

In vitro migration assay

Chemotaxis in response to chemoattractants was analyzed by measuring the number of cells migrating through a polycarbonate filter (8-μm pore size) in 24-well Transwell chambers (Costar). The upper chamber included 1–3 × 10^5 BMDCs in 100 μl chemotaxis medium (DMEM medium with 0.1% BSA and 10 mM HEPES), and the lower chamber contained 600 μl of the same medium with or without chemoattractants. After incubation for 3 h at 37°C, cells that migrated to the bottom chamber were stained with eFluor450 anti-CD11c (eBioscience) and analyzed for 1 min using LSRII flow cytometer and FACSDiva software (BD Biosciences). Numbers of CD11c$^+$ cells obtained in the lower chambers were divided by the number of CD11c$^+$ cells in the input samples and represented as percentage of input. In some experiments, cells were treated with 1 μg/ml exoenzyme C3 (cell-permeable form; Cytoskeleton) for 4 h before the migration assays. C3 was added or not to the upper chamber together with the cells.

DC retroviral infection

BMDCs were transfected by retroviral infection as described previously (14). Retrovirus was produced by transfecting Phoenix Eco 293T packaging cell line with SWAP-70–IRES–GFP or IRES-GFP. BMDCs were infected with retroviral supernatant at day 6. The plate was centrifuged at 1200 rpm at 24°C for 90 min and left overnight at 37°C. Virus was removed and DCs were reinfected with new retroviral supernatant. After 48 h of the second infection, CD11c$^+$ DCs were purified from cultures using anti-CD11c Abs bound to magnetic beads (Miltenyi Biotec) and activated overnight with LPS (1 μg/ml).

Time-lapse series of motile DC under an S1P concentration gradient

BMDCs were applied on a μ-slide for chemotaxis assay (ibidi) according to manufacturer's instructions. A total of 150 nM S1P was applied to create a concentration gradient. Time-lapse series of moving DCs were recorded every 2 min for 5 h on a Nikon live imaging station (Nikon) equipped with a 20× phase-contrast objective, automated X-Y-Z-stage, a climate chamber, and camera. Migration speed and directionality were analyzed with the Chemotaxis and Migration tool plug-in (ibidi) for ImageJ.

In vitro three-dimensional live cell imaging of DC morphology

Purified LPS-matured CD11c$^+$ BMDCs (3 × 10^5/ml) were kept in RPMI media (phenol red free; Invitrogen) containing 10% FCS and added to self-constructed imaging chambers with the glass bottom coated with a collagen mixture described previously for use in three-dimensional (3D) collagen matrices (24). Stimulation occurred with 100 nM S1P (Sigma). Imaging was performed on a CellR imaging workstation (Olympus, Hamburg, Germany) using an upright microscope stage (BX61) with a 60× (NA 0.9) water-coupled lens. Using an automated X-Y-Z-stage, we chose between 5 and 10 optical fields in each culture. Frame dimensions were 68 × 68 μm total. Images were taken every 20 s for up to 4 h with the transmitted light channel recorded. Images were processed with Virtualdub 1.8.6 and ImageJ 1.34s. For a total of 40 wt and *Swap70*$^{-/-}$ cells, mean dendrite length and number were quantified by measuring apparent dendrites at 5 consecutive time points with 240-sec interval for each cell.

Ear skin explant culture

Ears from wt or *Swap70*$^{-/-}$ animals were split into dorsal and ventral halves, and the cartilage-free half was cultured with medium in 24-well tissue culture plates for 24 or 48 h. Mechanical splitting of the ears is enough to trigger maturation of skin DCs (25). After incubation, ear halves were washed three times in PBS, fixed with methanol for 5 min, and incubated with PBS + 1% BSA before use for fluorescent labeling.

Confocal microscopy

For F-actin and Rho GTPases staining, LPS-matured BMDCs were left to adhere for 3 h on glass slides; then 50 nM S1P was added to the cells and left for 30 min. Cells were fixed with 3.7% paraformaldehyde in PBS for 10 min at room temperature. Cells were then blocked with 3% BSA in PBS and permeabilized with 1% Triton X-100 (Sigma) in PBS. Rac1 and RhoA staining was done with mAbs (Cytoskeleton) followed by Alexa Fluor 594-labeled Ab against mouse IgG (Invitrogen). Alexa Fluor 488-labeled phalloidin (Invitrogen) was used to visualize F-actin. Slides were mounted in Fluoromont-G (SouthernBiotech) and viewed using the Zeiss LSM 510 confocal microscopy system (Carl Zeiss). Imaging was performed using a 40×/1.3 differential interference contrast oil objective. Lasers of 488 and 561 nm were used for excitation of FITC and Alexa Fluor 594 respectively. Emissions wavelengths were separated by band passes 505–550 and >575 nm, respectively. Confocal sections of 1 μm/cell were taken. Colocalization of F-actin and Rho GTPases was quantified according to Ocaña-Morgner et al. (14). Forty cells were analyzed via ImageJ using the colocalization plug-in (ratio: 30%; threshold for each channel: 50). Nuclei were visualized with DAPI staining and an area around the cytoplasm of each cell in the colocalization image was analyzed for gray values representing the level of colocalization of two proteins (values close to the maximum of 256 represent strong colocalization). Profiles for each cell with a mean gray value per square micrometer were obtained, and the average of these mean values was plotted for Rac1–F-actin and RhoA–F-actin colocalization. Ears explant staining was done with goat polyclonal anti–LYVE-1 Abs (R&D Systems), FITC-labeled anti-murine Langerin/CD207 (Dendritics), FITC-labeled anti-CD86 (BD Biosciences), and Alexa 594-labeled anti-goat Abs (Invitrogen). The ear halves were mounted in Fluoromont-G (SouthernBiotech) and viewed using the Zeiss LSM 510 confocal microscopy system (Carl Zeiss). Imaging was performed using a 25×/0.8 differential interference contrast objective. Lasers of 488 and 561 nm were used for excitation of FITC and Alexa Fluor 594, respectively. Emissions wavelengths were separated by band passes 505–550 and >575 nm, respectively. Images were acquired using LSM 5Pas software (Carl Zeiss), analyzed by ImageJ (National Institutes of Health), and transferred to Photoshop 7.0 (Adobe Systems) to produce the final figures.

Skin FITC painting

Migration of skin DCs in foot pads was induced in vivo by applying 20 μl of 8 mg/ml FITC dissolved in a 50:50 (v/v) mixture of acetone and dibutylphthalate. After several time points, draining popliteal lymph node cell suspensions were analyzed for CD11c$^+$FITC$^+$ DCs by flow cytometry. Nondraining popliteal lymph nodes were used as control.

Endocytosis assay

LPS-mature BMDCs were incubated in DMEM with 0.5% BSA and 10 mM HEPES for 3 h at 37°C, then FITC-dextran (1 mg/ml) and S1P (100 nM)

Downloaded from http://www.jimmunol.org/ by guest on February 24, 2022

were added together and left incubating for 5 min. Endocytosis was stopped by placing the cells on ice. DCs were then washed three times with cold PBS containing 0.1% NaN_3. Mean fluorescence intensity of FITC-dextran$^+$ cells was analyzed by flow cytometer. Incubation of DCs with FITC-dextran and S1P at 4°C was used as negative control. In some experiments, cells were treated with 1 μg/ml exoenzyme C3 (cell-permeable form; Cytoskeleton) for 4 h before the migration assays. C3 was added or not to the lower chamber together with the chemoattractant.

Rho GTPases activity

The activities of Rho GTPases were analyzed using rhotekin-Rho– or PAK-rac/cdc42–binding domain agarose. Beads were subjected to SDS-PAGE and Western blotting with Abs against Rac1/2 (23A8; Upstate Biotechnology) and RhoA (119; Santa Cruz Biotechnology). Activity of Rho GTPases was quantified by densitometric analysis using ImageQuant software (Molecular Dynamics).

Purification of detergent-resistant membrane rafts

Membrane rafts were prepared by cell lysis of BMDCs followed by OptiPrep (Progen Biotechnik) gradient fractionation using ultracentrifugation as previously described (26). Five hundred-microliter fractions were collected from the top of the gradient. Protein concentration of each fraction was assayed by protein assay kit (Bio-Rad) based on the Bradford dye procedure. Fractions were analyzed individually by SDS-PAGE and Western blotting. Anti-caveolin 1 (Santa Cruz Biotechnology) and anti-transferrin receptor (Abcam) were used for positive and negative control of membrane rafts, respectively. Anti-$G\alpha_{12}$, anti-$G\alpha_{13}$, and anti-$G\alpha_I$ (all from Santa Cruz Biotechnology) were also used.

Immunoprecipitation

LPS-treated wt BMDCs were stimulated with 50 nM S1P for 30 min. A total of 2×10^7 DCs were incubated on ice for 10 min in hypertonic buffer (250 mM sucrose, 10 mM Na-HEPES pH 7.2, 2 mM $MgCl_2$, 10 mM NaF) that was freshly supplemented with a protease inhibitor mixture. Cells were lysed twice in a nitrogen cavitation apparatus at 1000 pounds per square inch for 7 min each. The soluble cell lysates were mixed with 1 μg polyclonal anti–SWAP-70. Cell lysates were rocked overnight at 4°C. Protein G Sepharose beads were added and rocked for 1 h. The beads were washed three times with the hypertonic buffer and the precipitates analyzed by SDS-PAGE, followed by immunoblotting using anti–SWAP-70 or anti-Rho GTPase Abs.

Statistical analysis

For direct comparison of the activity of wt and *Swap70*$^{-/-}$ cells, statistical significance was determined with the Mann–Whitney *U* test for two-tailed data. The *p* values <0.05 were considered highly significant.

Results

Swap-70$^{-/-}$ *BMDCs are impaired in S1P-induced motility*

In mature DCs, motility is enhanced by S1P signaling mainly through $S1P_1$ and $S1P_3$ (8, 11, 12). Transwell chemotaxis assays showed that *Swap-70*$^{-/-}$ BMDCs are significantly reduced in their S1P-induced motility at every effective S1P concentration tested as compared with wt (Fig. 1*A*). This difference was observed for both BMDCs (Fig. 1*A*) and spleen-derived DCs (data not shown). Motility of immature DCs was not different from that seen without S1P and was similar in wt and *Swap-70*$^{-/-}$ BMDCs (data not shown). Motility tests using other chemoattractants, that is, CCL19 or CCL21, showed no difference in the response of *Swap-70*$^{-/-}$ or wt BMDCs (Fig. 1*A*), indicating specificity of SWAP-70 for S1P signaling. To confirm the SWAP-70 dependency of the S1P-mediated chemotactic response phenotype, we introduced a SWAP-70–IRES–GFP retroviral expression construct (14) into SWAP-70–deficient BMDCs. Expression of SWAP-70 in *Swap-70*$^{-/-}$ BMDCs restored their S1P response to levels comparable with wt cells (Fig. 1*B*). In wt BMDCs, expression of SWAP-70, as well as infection by the empty control vector itself, stimulated their migration when compared with mock-treated control cells. Transduction of DCs with retroviral vectors leads to some activation (27), which may be reflected in the improved capacity to migrate to S1P in wt BMDCs. Thus, activation is not sufficient to rescue the migration deficiency in *Swap-70*$^{-/-}$ BMDCs.

The speed of motility was also reduced in response to an S1P concentration gradient as seen by analysis of time-lapse movies of *Swap-70*$^{-/-}$ and wt BMDCs on two-dimensional (2D) surfaces (Fig. 1*C*, Supplementary Videos 1, 2). There was no difference between wt and *Swap-70*$^{-/-}$ BMDCs in response to CCL19 or CCL21 in these assays (not shown). Directionality toward S1P, however, was not affected in *Swap-70*$^{-/-}$ BMDCs (Fig. 1*C*). Analysis of individual cells in response to an S1P concentration gradient on 2D surfaces showed no significant difference in morphology (data not shown). The morphology of cells in response to S1P in a 3D environment was investigated next. In this study, motility is driven by cytoskeleton dynamics, that is, flow of actin polymerization at the cell front and actomyosin contractions of the trailing edge to propel the nucleus through narrow spaces (17). A deficiency in DCs to properly move through 3D environments, which to some extent reflect the interstitial space in the skin, was previously reported to result in deficient migration to lymph nodes (17, 18). Morphological analyses of wt cells showed a round cell body with the nucleus mostly close to the body center. Their dendrites were usually not very long and they spread around the entire cell body (circular dendrites) most of the time (Fig. 1*D*, Supplemental Video 3). *Swap-70*$^{-/-}$ BMDCs, in contrast, showed a more elongated morphology; the cell body was more stretched out and the nucleus often lagging behind. In addition, the dendrites of *Swap-70*$^{-/-}$ BMDCs were significantly longer when compared with wt BMDCs, whereas there was no difference in number of dendrites (Fig. 1*D*, Supplemental Video 4).

Delayed entry into lymphatic vessels and migration to lymph nodes of Swap-70$^{-/-}$ *DCs*

Recent studies indicate that S1P does not regulate migration of DCs from the periphery to lymph nodes under steady-state conditions (11, 28). However, this situation may change under local or systemic inflammatory conditions (8). In addition, S1P regulation of migration of DCs in vivo is indicated by studies with S1P agonists and S1P receptor knockout mice where S1P controls migration of mature DCs from skin, lung, or lamina propria to draining lymph nodes (4–8). The morphology of *Swap-70*$^{-/-}$ BMDCs on 3D collagen matrix indicated a defect in dragging the nucleus through small pores. This deficiency may reflect impaired migration of skin *Swap-70*$^{-/-}$ DCs through interstitial space likely resulting in impaired entry into lymphatic vessels in the skin (17). To test this, we studied entry of DCs into lymphatic vessels by analyzing the migration of DCs in the skin of ear explants. Mechanical splitting of ears into halves followed by incubation in medium at 37°C triggered activation of DCs and their migration into lymphatic vessels, which were visualized by LYVE-1 staining (5). CD86 and Langerin were used as markers for skin DCs (5). We did not use MHC-II as a marker because of the MHC-II phenotype in *Swap-70*$^{-/-}$ BMDCs previously described (14). Vessel morphology and intervessel distance were the same in wt and *Swap-70*$^{-/-}$ ears. CD86$^+$- and Langerin$^+$- *Swap-70*$^{-/-}$ DCs showed significantly delayed entry into lymphatic vessels as compared with wt (Fig. 2*A*). Thus, *Swap-70*$^{-/-}$ DCs were impaired in their entry into skin lymphatic vessels in vivo. We also observed that Langerin$^+$ DCs generally entered lymphatic vessels later than the majority of CD86$^+$ cells. This probably is due to the fact that Langerin$^+$ DCs, which are mostly epidermal, are known to enter lymphatic nodes after dermal DCs (25, 29, 30). Entry of DCs into lymphatic vessels also depends on adhesion molecules on DCs that interact with ligands on lymphatic endothelial cells (31, 32). Lymphatic entry

Downloaded from http://www.jimmunol.org/ by guest on February 24, 2022

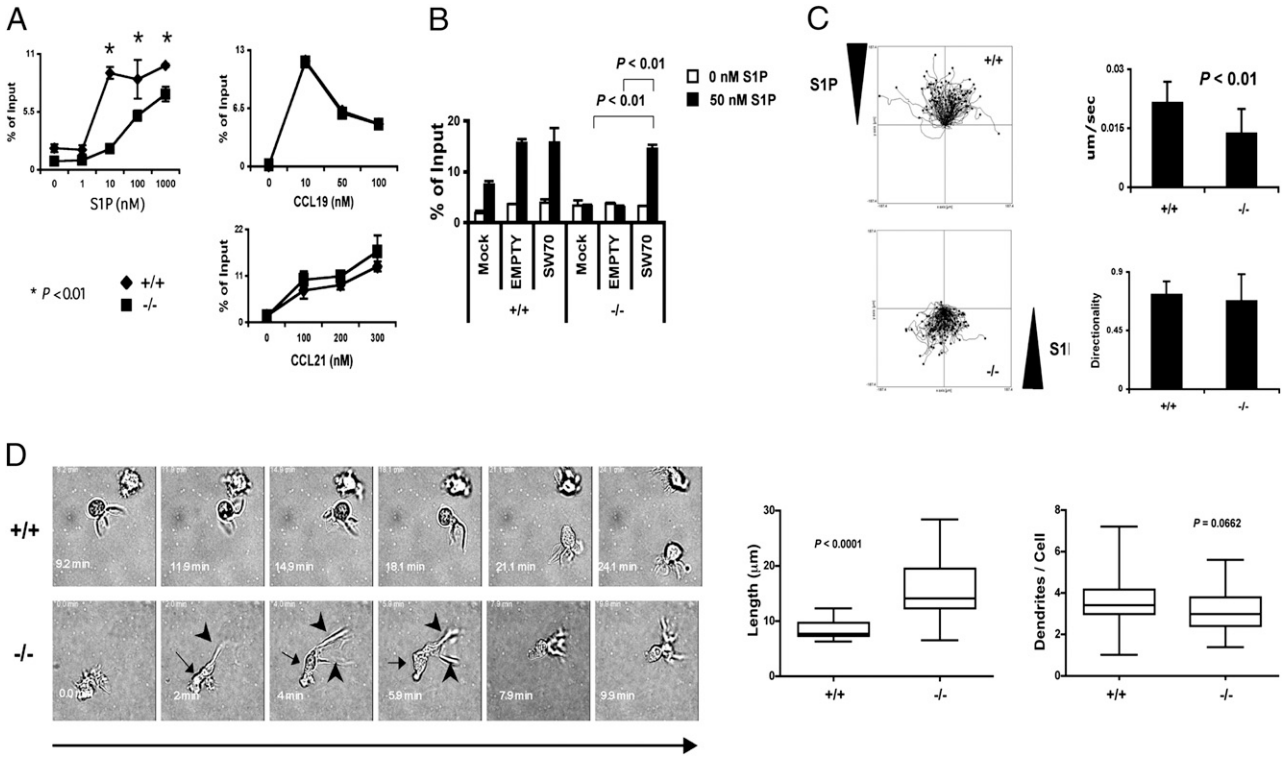

FIGURE 1. Impaired motility response to S1P by *Swap-70*$^{-/-}$ BMDCs. *A*, In vitro migration assays of LPS-activated *Swap-70*$^{-/-}$ and wt BMDCs in response to S1P (*top left panel*), CCL19 (*top right panel*), or CCL21 (*bottom left panel*). Migration is calculated as percentage of input after 3-h exposure to different concentrations of the chemoattractants in a Transwell system. Data are representative of at least 10 independent experiments. *B*, In vitro migration assays of LPS-activated *Swap-70*$^{-/-}$ and wt BMDCs in response to S1P after retroviral infection used for the expression of SWAP-70. Mock treatment and empty retroviral vector were used as control. Migration is calculated as percentage of input after 3-h exposure to 50 nM S1P in a Transwell system. *C*, Quantification of time series after live cell imaging in response to an S1P gradient using ibidi μ-slide shows velocity (μm/sec) and directionality. Images were taken every 2 min for up to 5 h. Videos were analyzed with the Chemotaxis and Migration tool plug-in (ibidi) for ImageJ. *D*, In vitro 3D live cell imaging of DC morphology. LPS-matured and MACS-purified CD11c$^+$ BMDCs (3×10^5/ml) were added to self-constructed imaging chambers with the glass bottom coated with a collagen mixture. Stimulation occurred with 100 nM S1P. Images were taken every 20 s for up to 4 h. *Swap-70*$^{-/-}$ BMDCs show a more elongated body shape with the nucleus dragging behind (arrows) and long dendrites (arrowheads). Dendrite length (*left panel*) and number (*right panel*) were determined for a total of 40 wt and *Swap70*$^{-/-}$ cells. Data are representative of at least three independent experiments.

defect in the skin may reflect an impairment of *Swap-70*$^{-/-}$ DCs to transmigrate through lymphatic endothelial cells. To address this, we tested the chemotactic response of wt and *Swap-70*$^{-/-}$ BMDCs to CCL19 in a modified Transwell system where the porous membranes were coated with the C3H/HeJ mouse endothelial line SVEC4-10 that is reported as lymphatic endothelial cells (33). Although the transmigration through the endothelial cells greatly improved the chemotactic response to CCL19 of wt cells, the magnitude of the *Swap-70*$^{-/-}$ BMDCs response was significantly lower (Supplemental Fig. 1*A*). We observed the same deficiency to transmigrate in *Swap-70*$^{-/-}$ BMDCs when S1P was used as chemoattractant (Supplemental Fig. 1*B*). SWAP-70–deficient B cells have impaired entry to lymph nodes from the blood (34). During this process, *Swap70*$^{-/-}$ B cells aberrantly regulated integrin-mediated adhesion to blood endothelial cells (34). To address the role of integrins in the transmigration defect of *Swap-70*$^{-/-}$ BMDCs, we performed the same experiments as in Supplemental Fig. 1*A* in the presence of different concentrations of either EDTA or a blocking Ab against integrin β_2, which has been reported to regulate transmigration of DCs (31, 32). Although EDTA and the anti-β_2 Ab had an immediate negative effect on wt BMDCs, it took concentrations of up to 1000× (EDTA) or 500× (anti-β_2) higher to have an effect on *Swap-70*$^{-/-}$ BMDCs (Supplemental Fig. 1*C*). A blocking Ab against VCAM did not have an effect on either wt or *Swap-70*$^{-/-}$ DCs. These results indicate defective integrin signaling in *Swap-70*$^{-/-}$ BMDCs, and future studies will be done to characterize the integrin-mediated adhesion to lymphatic endothelial cells in *Swap-70*$^{-/-}$ BMDCs.

Skin-resident DCs require $S1P_1$ for efficient migration into the draining lymph node (8). We analyzed in vivo migration of DCs by FITC painting of foot pads of *Swap-70*$^{-/-}$ and wt mice followed by analysis of FITC$^+$CD11c$^+$ cells in the draining lymph nodes after 24, 48, and 72 h. Although we observed a decrease in the percentage of FITC$^+$CD11c$^+$ cells in the draining lymph nodes of wt animals as time increases after painting, the percentage of cells in *Swap-70*$^{-/-}$ animals actually increased to reach similar levels as wt DCs at 24 h (Fig. 2*B*). The failure to migrate early to lymph nodes in *Swap-70*$^{-/-}$ mice was not due to reduced numbers of DCs in the skin of the animals, because microscopic analysis and cell isolation procedures did not reveal a difference between wt and *Swap-70*$^{-/-}$ mice in the number of skin DCs (Supplemental Fig. 1*D*, left panel, and data not shown). As already suggested by data shown in Fig. 2*A*, these results indicate delayed migration of skin-resident DCs to draining lymph nodes in *Swap-70*$^{-/-}$ mice. The assays used in this set of experiments represent inflammatory conditions (35), but under steady-state, *Swap-70*$^{-/-}$ animals also show significantly decreased percentage and total numbers of DCs in lymph nodes (Supplemental Fig. 1*D*, right panels); MHC-II$^-$ cells, considered quiescent resident cells (24), are not changed. This indicates a mechanism, controlled by SWAP-70, that is shared for migration of DCs under steady-state and inflammatory conditions, and shall be the subject of further studies.

Downloaded from http://www.jimmunol.org/ by guest on February 24, 2022

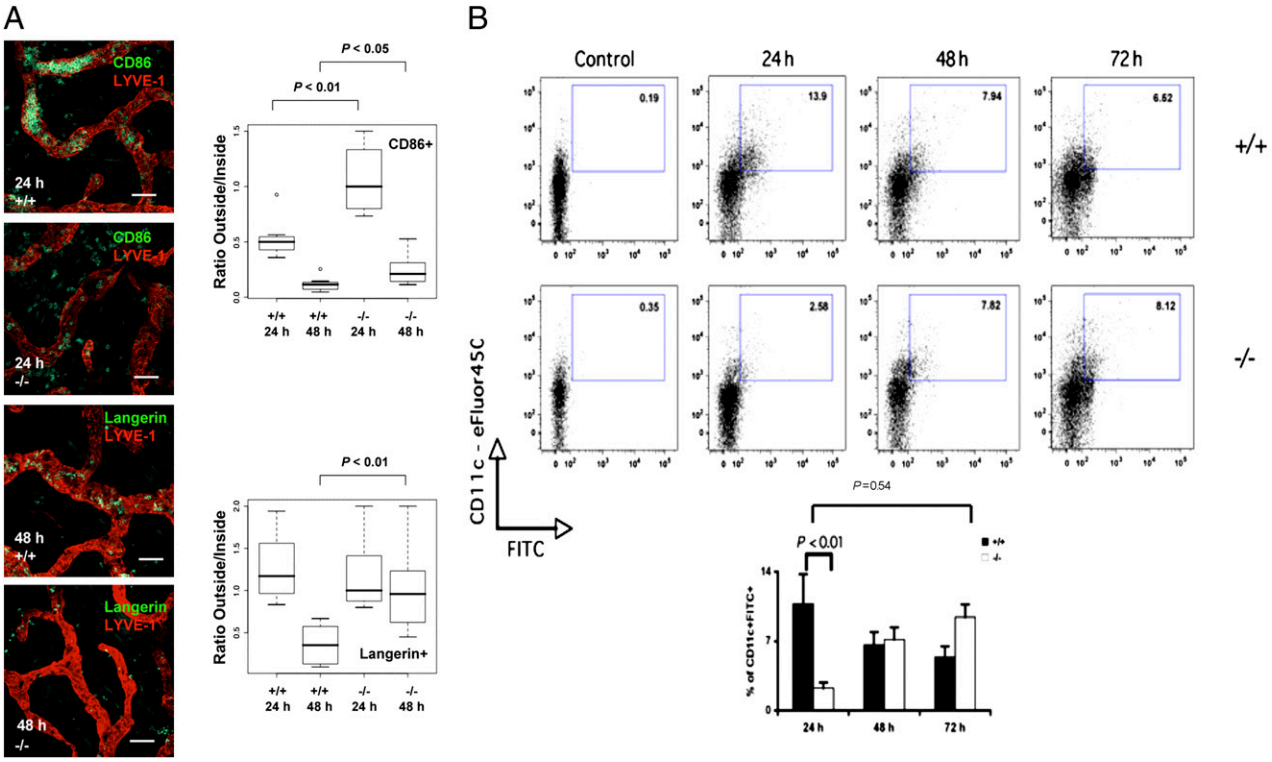

FIGURE 2. Delayed entry of *Swap-70*$^{-/-}$ DCs to lymphatic vessels and migration to lymph nodes. *A*, Confocal microscopy analysis of localization of CD86^{+} and Langerin^{+} cells outside or inside LYVE1^{+} lymphatic vessels of ear explants after 24- or 48-h incubation at 37°C. CD86^{+} and Langerin^{+} cells were counted in each picture of ears, and the number of cells outside LYVE1^{+} lymphatic vessels were plotted against the number of cells inside. Scale bars, 100 μm. *B*, FITC painting of foot pads. *Swap-70*$^{-/-}$ and wt animals were painting in one foot pad with 8 mg/ml FITC dissolved in a 50:50 (v/v) mixture of acetone and dibutylphthalate. After 24 h, draining popliteal lymph nodes were isolated and analyzed for CD11c^{+}FITC^{+} DCs by flow cytometry. Popliteal lymph nodes from nonpainted foot pads were used as control. Data are representative of at least three independent experiments.

Expression of S1P receptors is unaltered in Swap-70$^{-/-}$ *BMDCs*

Using real-time PCR, we analyzed the expression of mRNA of the S1P receptors known to control DC motility and endocytosis in response to S1P, that is, $S1P_1$ and $S1P_3$ (11, 12), and of $S1P_2$. mRNA levels of these three receptors were not significantly different in *Swap-70*$^{-/-}$ or wt BMDCs at several time points after incubation with LPS (Table I). In agreement with previous reports, we observed upregulation of mRNA levels $S1P_1$ and $S1P_3$ and downregulation of $S1P_2$ (4, 8, 11). At the protein level, determination of expression of the receptors $S1P_1$ and $S1P_3$ by flow cytometry on the surface of LPS-stimulated *Swap-70*$^{-/-}$ or wt BMDCs did not show significant differences (Fig. 3). These results indicated that SWAP-70 might control signaling in response to S1P after binding to the receptors in mature DCs rather than receptor expression.

Defective S1P-induced endocytosis of Swap-70$^{-/-}$ *BMDCs*

In vitro, S1P enhances endocytosis in LPS-mature BMDCs, but not in immature BMDCs, through $S1P_3$ signaling (11, 36). This would constitute a mechanism thought to promote the rapid removal of pathogens at sites of infection (11, 36). To test this, we studied the effect of S1P on the endocytosis of LPS-matured BMDCs. After 5 min of exposure to S1P, endocytosis of FITC-dextran particles was significantly increased in wt BMDCs. In contrast, *Swap-70*$^{-/-}$ BMDCs failed entirely to enhance endocytosis of FITC-dextran (Fig. 4). Endocytosis is affected by the endosome transport inside cells that is mainly controlled by activation of RhoB (37, 38). We previously reported reduced expression of total RhoB during stimulus with LPS of *Swap-70*$^{-/-}$ BMDCs (14). However, the level of active RhoB-GTP remained the same in *Swap-70*$^{-/-}$ BMDCs after LPS addition (14). We excluded that the defect in S1P-induced endocytosis is due to failure to activate RhoB in

Table I. mRNA expression pattern of $S1P_1$, $S1P_2$, and $S1P_3$ in inactivated (LPS^{-}) and activated (LPS^{+}) DCs

BMDCs	$S1P_1$ (Mean ± SEM)	$S1P_2$ (Mean ± SEM)	$S1P_3$ (Mean ± SEM)
wt			
LPS^{-}	0.0009 ± 0.0001	0.0015 ± 0.0001	0.0001 ± 9.76E-05
LPS^{+}	0.0025 ± 0.0003	0.0008 ± 0.0002	0.0046 ± 0.0003
SWAP-70$^{-/-}$			
LPS^{-}	0.0009 ± 0.0001	0.0014 ± 0.0002	0.0002 ± 0.0001
LPS^{+}	0.0021 ± 0.0003	0.0007 ± 0.0002	0.0039 ± 0.0006

Real-time quantitative PCR analysis of wt and *SWAP-70*$^{-/-}$ BMDCs was performed as described in *Materials and Methods*. The amount of product for each PCR was normalized to GAPDH (mean ± SEM of a representative experiment).

Downloaded from http://www.jimmunol.org/ by guest on February 24, 2022

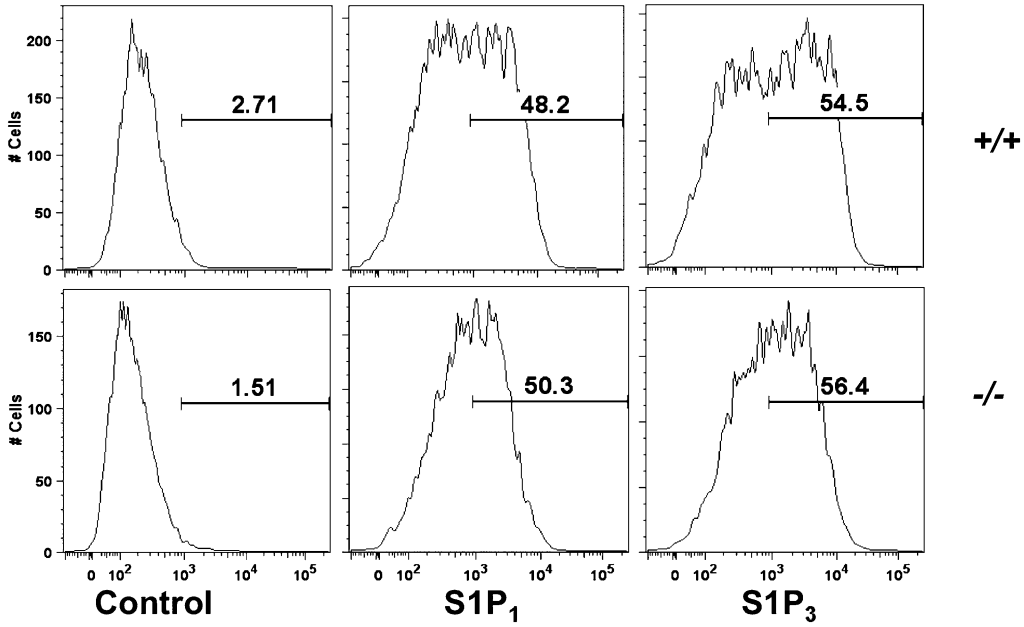

FIGURE 3. Expression of receptors $S1P_1$ and $S1P_3$ on the surface of LPS-stimulated wt (*top panels*) and *Swap-70*$^{-/-}$ BMDCs (*lower panels*). Secondary Ab anti-rabbit IgG was used as control. Data are representative of at least three independent experiments.

Swap-70$^{-/-}$ BMDCs because we do not observe any difference in the activation of RhoB after S1P stimulus in LPS-treated wt and *Swap-70*$^{-/-}$ BMDCs (data not shown). Furthermore, we did not find differences in endocytosis of immature wt and *Swap-70*$^{-/-}$ BMDCs (data not shown). These and the earlier data demonstrate an impaired S1P response in LPS-mature *Swap-70*$^{-/-}$ BMDCs that results in a failure to activate important functions, that is, motility and endocytosis.

SWAP-70 interacts with $G\alpha_I$ in BMDC extracts, and Swap-70$^{-/-}$ BMDCs fail to localize $G\alpha_{13}$ in membrane rafts

Previously, we reported interaction of SWAP-70 with the active forms of Rac1 and RhoA in BMDC lysates (14). This interaction may account for the proper activation and localization of these Rho GTPases after S1P stimulus. Failure of S1P signaling in *Swap-70*$^{-/-}$ DCs may also suggest interaction of SWAP-70 with other members upstream of Rho GTPases, for example, S1P receptors, G proteins, or both. We tested whether SWAP-70 interacts with S1P receptors and Gα proteins. We performed immunoprecipitation assays of cells after S1P stimulus. Lysates were obtained after incubation of cells with hypertonic buffer followed by lysis with nitrogen cavitation to preserve receptors complex that may form at the membrane, which otherwise would be disrupted in lysates prepared with detergents. We found that in wt BMDCs lysates, SWAP-70 interacts strongly with $G\alpha_I$ and, to a lesser level, with $G\alpha_{13}$ (Fig. 5*A*). We did not detect interaction with $S1P_3$ (Fig. 5*A*) or $S1P_1$ (data not shown). To test whether this interaction depends on intact membrane fragments where the proteins may associate, but not necessarily directly interact, we performed immunoprecipitation in detergent-containing lysis buffers. We observed interaction of SWAP-70 with $G\alpha_I$, but not with $G\alpha_{13}$, when the detergent NP-40 was used (Supplemental Fig. 2). However, this interaction disappeared when octyl glucoside was used, a detergent known to dissociate membranes and their associated proteins (39) (Supplemental Fig. 2). Together, these results show direct or membrane domain-mediated interactions of SWAP-70 with $G\alpha_I$ proteins.

S1P GPCRs and their signaling components, for example, Gα proteins, can be compartmentalized in membrane rafts and caveolae to initiate receptor-specific signal transduction (see Refs. 40, 41 for review). We analyzed the membrane localization of Gα proteins that are responsible for Rho GTPases activation after S1P stimulus (10). Fig. 5*B* shows that, in both immature wt BMDCs and *Swap-70*$^{-/-}$ BMDCs, $G\alpha_I$ and $G\alpha_{13}$ localized in membrane rafts/caveolae, which were identified by the use of caveolin 1. However, after LPS stimulus, $G\alpha_{13}$ disappeared from the membrane rafts/caveolae fractions of *Swap-70*$^{-/-}$ BMDCs, whereas it largely remained in the corresponding wt fractions. The same relocalization events happened in BMDCs stimulated by LPS and S1P. In wt BMDCs, a relatively large portion of $G\alpha_{13}$ localized to membrane rafts/caveolae (gradient fraction no. 2) compared with the portion of $G\alpha_{13}$ appearing in the heavy fractions (no. 5, 6). In addition, the Rac activator $G\alpha_i$ was lost from raft fractions in wt and *Swap-70*$^{-/-}$ BMDCs on LPS or LPS/S1P stimulation (Fig. 5*B*). Our initial data on failure of MHC-II localization into lipid

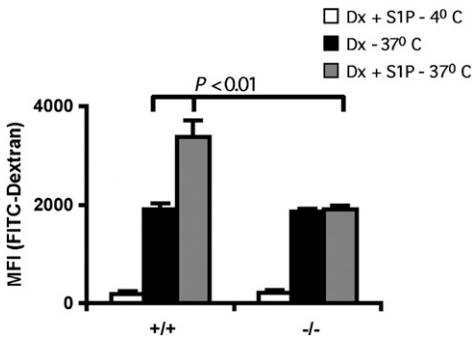

FIGURE 4. Deficient S1P-induced endocytosis of *Swap-70*$^{-/-}$ BMDCs. After serum starvation, LPS-matured BMDCs were incubated with 1 mg/ml FITC-dextran in the presence or absence of 100 nM S1P for 5 min at 37°C. After incubation, cells were analyzed by flow cytometry to determine the FITC mean fluorescence intensity (MFI). Incubation at 4°C was used as negative control. Data are representative of at least three independent experiments.

Downloaded from http://www.jimmunol.org/ by guest on February 24, 2022

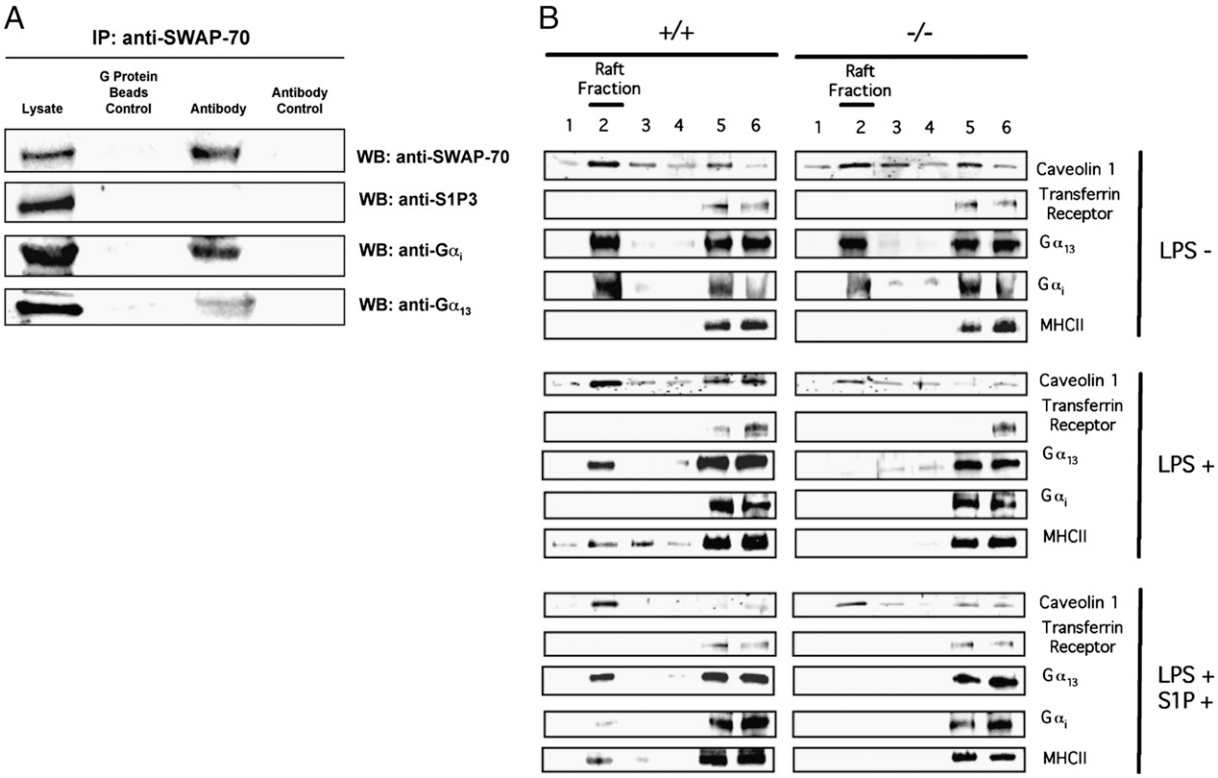

FIGURE 5. SWAP-70 interacts with $G\alpha_I$ in BMDC extracts and *Swap-70*$^{-/-}$ BMDCs fail to localize $G\alpha_{13}$ in membrane rafts. *A*, *Swap-70*$^{+/+}$ BMDCs lysates were immunoprecipitated with polyclonal anti–SWAP-70. Complexes were analyzed by Western blotting with anti–SWAP-70, anti-$S1P_3$, anti-$G\alpha_I$, and anti-$G\alpha_{13}$. *B*, Lysates of immature (LPS^-), LPS-matured (LPS^+), or LPS-S1P–matured (LSP^+S1P^+) BMDCs were subjected to OptiPrep gradient ultracentrifugation system. After centrifugation, six fractions were collected from the top of the tube, resolved by SDS-PAGE, and analyzed by Western blotting. Membranes were probed with polyclonal Ab against caveolin 1 for localization of membrane rafts and polyclonal Ab against transferring receptor as negative control.

rafts (14) were reproduced using additional markers such as caveolin 1 (Fig. 5*B*). Unlike in wt BMDCs, lipid raft formation is inefficient in *Swap-70*$^{-/-}$ BMDCs, as is formation of caveolin-positive membrane fractions. Thus, SWAP-70 is involved in control of formation of membrane domains like lipid rafts.

Swap-70$^{-/-}$ *BMDCs fail to activate RhoA and to localize Rac1 and RhoA to areas of F-actin on S1P treatment*

DC motility is enhanced by stimulation of $S1P_1$ and $S1P_3$ (5, 8, 11, 12), whereas endocytosis is mainly mediated through $S1P_3$ signaling (11). Previously, it was demonstrated that migration of mature DCs toward S1P depends on cytoskeleton-associated activation of Rho GTPases Rac1 and RhoA (4). $S1P_1$ activates Rac1, whereas $S1P_3$ activates Rac1 and RhoA (10). Thus, we studied the activation of Rac1 and RhoA in LPS-matured BMDCs after addition of S1P. *Swap-70*$^{-/-}$ BMDCs failed to activate RhoA and rather did not maintain its basal activation level (Fig. 6*A*). In contrast, activated Rac1 in *Swap-70*$^{-/-}$ BMDCs was not significantly different from wt BMDCs (Fig. 6*B*).

The role of RhoA activation in the chemotactic response to S1P of mature DCs was assayed using the exoenzyme C3 ADP-ribosyltransferase from *Clostridium botulinum*, which ADP-ribosylates and thus inactivates RhoA, but not Rac1 or Cdc42 (42). Although *Swap-70*$^{-/-}$ BMDCs were low in migration anyway, inactivation of RhoA during the transwell chemotaxis assays strongly inhibited migration to S1P of wt BMDCs (data not shown), indicating that RhoA plays an active role during migration to S1P in DCs in agreement with previous studies (4). In contrast, migration to CCL19 and CCL21 was not affected (data not shown), agreeing with previous data where RhoA inactivation with exoenzyme C3 did not inhibit CCR7-mediated migration of human DCs (43).

Rho GTPases colocalize with centers of actin polymerization as cells migrate in response to extracellular stimuli (44). Rho GTPases localize to F-actin structures that control migration in cells (45, 46). Colocalization analysis by confocal microscopy of Rac1 in F-actin areas in wt BMDCs on stimulation with S1P shows significantly more localization of the two proteins in the same areas (Fig. 6*C*), as shown by the levels of gray values representative of colocalization (Fig. 6*D*, 6*E*). There was a modest, albeit significant, increase in the level of localization of RhoA in F-actin areas in wt BMDCs after S1P stimulus (Fig. 6*C–E*). *Swap-70*$^{-/-}$ BMDCs fail to increase the level of localization of either Rac1 or RhoA with F-actin areas (Fig. 6*C–E*). In addition, the level of localization between RhoA and F-actin is significantly greater in *Swap-70*$^{-/-}$ BMDCs than in their wt counterparts before S1P stimulus (Fig. 6*D*, 6*E*). This agrees with the higher content of active RhoA, that is, RhoA-GTP, in unstimulated *Swap-70*$^{-/-}$ BMDCs (Fig. 6*A*). Taken together, these results show that *Swap-70*$^{-/-}$ BMDCs are impaired in their ability to properly activate and localize Rac1 and RhoA after S1P stimulus.

Preinhibition of RhoA restores S1P-induced motility, endocytosis, and localization of $G\alpha_{13}$ *in membrane rafts in Swap-70*$^{-/-}$ *BMDCs*

In nonactivated, immature *Swap-70*$^{-/-}$ BMDCs, RhoA is constitutively active, and this activation can be inhibited by pretreatment of the cells with exoenzyme C3 (14). In this study, we observed that in LPS-matured *Swap-70*$^{-/-}$ BMDCs, RhoA was also significantly more active than in wt BMDCs (Fig. 6*A*). We

Downloaded from http://www.jimmunol.org/ by guest on February 24, 2022

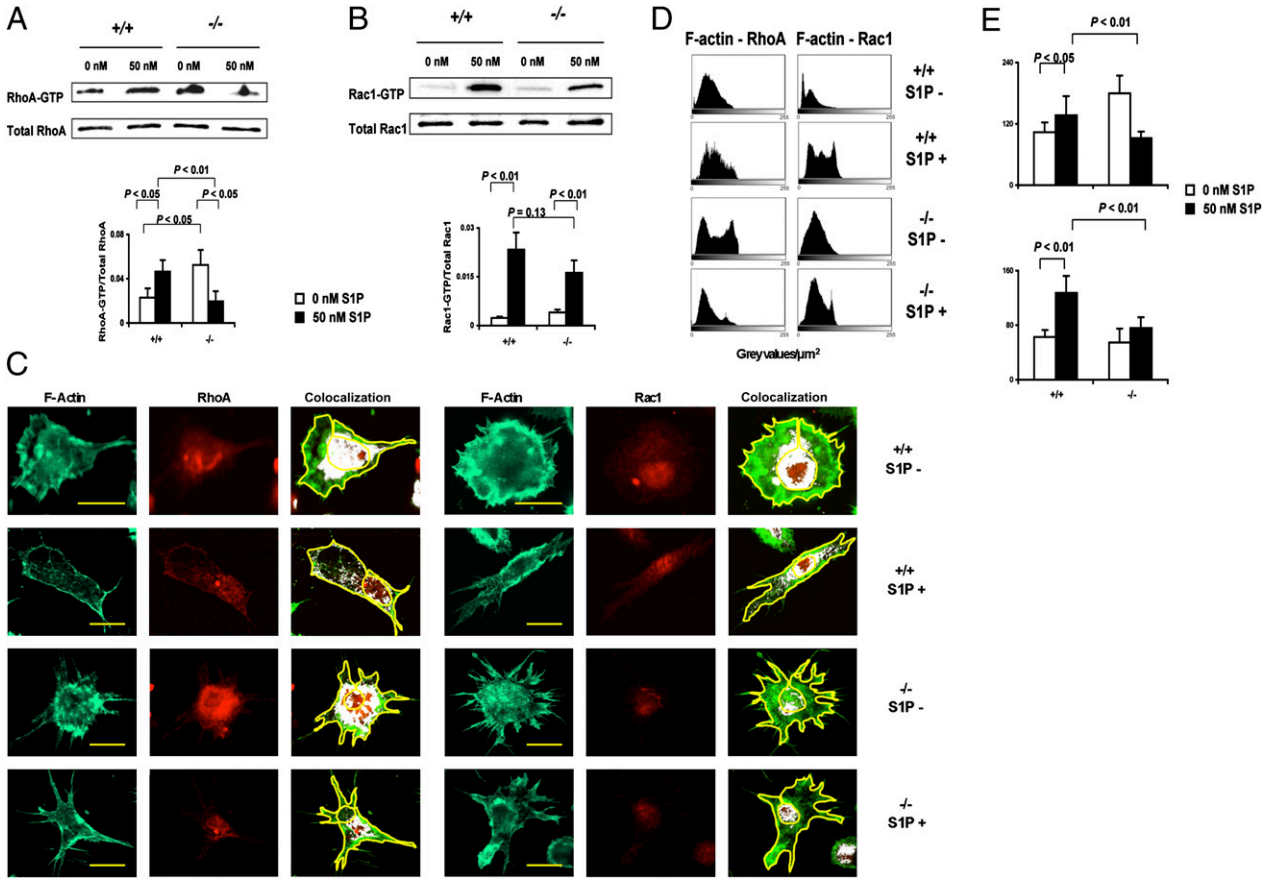

FIGURE 6. *Swap-70*$^{-/-}$ BMDCs fail to activate RhoA and to localize Rac1 and RhoA to areas of F-actin on S1P treatment. *A* and *B*, Activation of Rho GTPases in LPS-activated BMDCs after S1P stimulus was analyzed using (*A*) rhotekin-Rho–binding domain or (*B*) PAK-Rac/Cdc42–binding domain agarose beads. Beads were then subjected to SDS-PAGE and Western blotting. Activity of Rho GTPases was quantified by densitometric analysis and expressed as ratio of activated to total Rho GTPases. *C–E*, Localization of RhoA and Rac1 into F-actin areas in wt and *Swap-70*$^{-/-}$ BMDCs. *C*, Colocalization images show gray spots representing localization of the two proteins in F-actin areas. An area around the cytoplasm (yellow line) was drawn for quantification of gray values. Scale bars, 10 μm. *D*, Histograms show the distribution of gray values per square micrometer for the colocalization images used in *C*. *E*, Average of the mean gray values per square micrometer obtained from all of the histograms (40 for each staining) analyzed for RhoA (*upper panel*) and Rac1 (*lower panel*). Data are representative of at least 2 independent experiments, each with 40 cells measured.

preincubated LPS-matured BMDCs with exoenzyme C3 before performing S1P chemotaxis transwell and endocytosis assays. The cells were washed thoroughly before performance of the assays. Restoration of Rho GTPase activity is known to occur within 3 h after removal of the drug (42). Such treatment restored *Swap-70*$^{-/-}$ BMDC migration to S1P to levels close to wt cells (Fig. 7*A*). The same treatment inhibited to some degree migration of wt cells as well, indicating that there was some remaining inhibitory effect of the exoenzyme (Fig. 7*A*). Preinhibition of RhoA also restored the capacity of *Swap-70*$^{-/-}$ BMDCs to upregulate endocytosis after S1P triggering (Fig. 7*B*). In contrast, wt cells lost the ability to upregulate endocytosis, suggesting that RhoA activation was required for upregulation of S1P-mediated endocytosis (Fig. 7*B*). Moreover, localization of $G\alpha_{13}$ in membrane rafts in *Swap-70*$^{-/-}$ DCs was seen at the same level as in wt BMDCs when RhoA was preinhibited (Fig. 7*C*). Inactivation of RhoA by exoenzyme C3 before and during S1P stimulus in *Swap-70*$^{-/-}$ and wt BMDCs was tested by using pull-down assays with rhotekin-Rho–binding domain agarose (Supplemental Fig. 3). These results indicated that SWAP-70 ensures regulated and timely activation of RhoA in mature DCs, thereby allowing proper S1P signaling.

Discussion

S1P signaling through its receptors constitutes an important mechanism to enhance motility and endocytosis of mature DCs (4, 5, 8, 11, 12). In this article, we identify SWAP-70 as a new factor controlling S1P signaling in mature DCs. *Swap-70*$^{-/-}$ BMDCs showed deficient upregulation of motility and endocytosis in response to S1P. Migration to S1P was restored by re-expression of SWAP-70 in *Swap-70*$^{-/-}$ BMDCs. Morphological analysis in a 3D collagen matrix under S1P stimulus showed a deficiency of *Swap-70*$^{-/-}$ BMDCs to migrate through small pores. Reduced motility to S1P of *Swap-70*$^{-/-}$ BMDCs in 2D and 3D environments correlated with delayed entry into lymphatic vessels and migration to lymph nodes of skin *Swap-70*$^{-/-}$ DCs. Migration of mature DCs to S1P depends on the simultaneous activity of the GTPases Rac1 and RhoA (4), and our study shows that inhibition of RhoA activation abolished the upregulation of endocytosis in wt BMDCs. However, the analysis of Rho GTPase activation in mature *Swap-70*$^{-/-}$ BMDCs demonstrated that they contained a significantly greater level of active RhoA, and that they failed to upregulate active RhoA after an S1P stimulus. In this study, we found for the first time, to our knowledge, an interaction of SWAP-70 with the S1P signaling proteins $G\alpha_I$. These interactions may be direct, but as a membrane-solubilizing detergent dissociates them, the interaction may depend on the membrane; thus, SWAP-70 may colocalize with the G proteins in a membrane signaling cluster. This hypothesis fits to the observation that *Swap-70*$^{-/-}$ BMDCs failed to localize the signaling proteins $G\alpha_{13}$ required for RhoA activation to membrane rafts/caveolae. Together,

Downloaded from http://www.jimmunol.org/ by guest on February 24, 2022

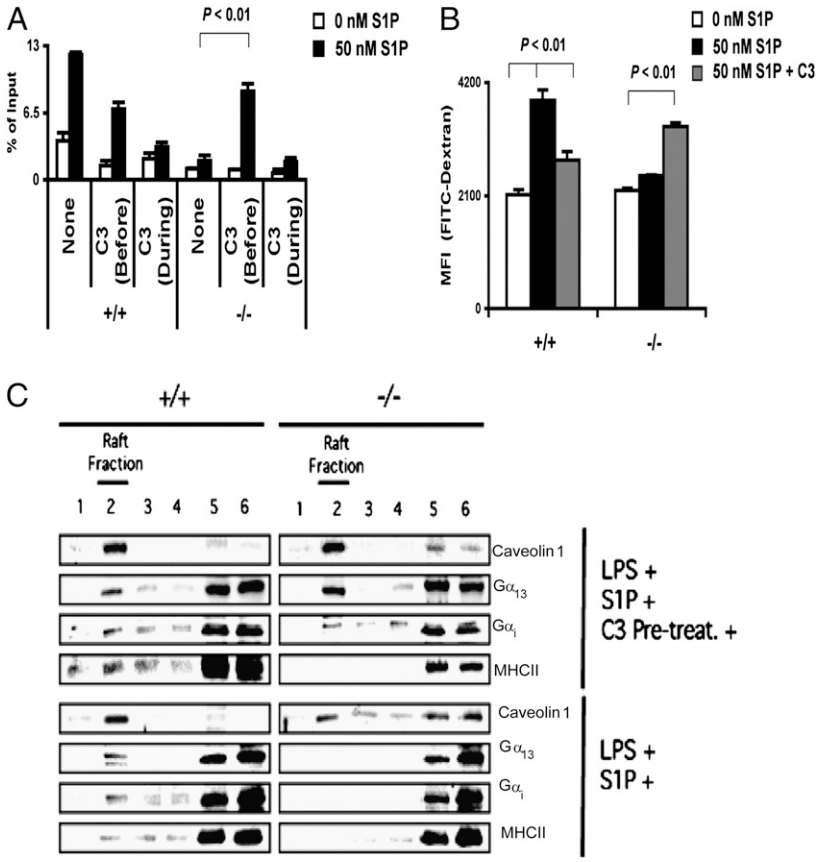

FIGURE 7. Preinhibition of RhoA activation increases the S1P-induced motility, endocytosis, and localization of $G\alpha_{13}$ in membrane rafts in *Swap-70*$^{-/-}$ BMDCs. *A*, LPS-activated *Swap-70*$^{-/-}$ and wt BMDCs were treated with exoenzyme C3 before or during in vitro migration in response to S1P. Migration is calculated as percentage of input after 3-h exposure to 50 nM S1P in a transwell system. *B*, LPS-activated *Swap-70*$^{-/-}$ and wt BMDCs were treated with 1 μg/ml exoenzyme C3 for 4 h before in vitro endocytosis in the presence or not of 100 nM S1P. Cells were analyzed by flow cytometry to determine the FITC mean fluorescence intensity (MFI). *C*, LPS-activated *Swap-70*$^{-/-}$ and wt BMDCs were treated or not with exoenzyme C3 for 4 h before S1P stimulus. Lysates of DCs were subjected to OptiPrep gradient ultracentrifugation system and analyzed as in Fig. 5*B*. Data are representative of at least three independent experiments.

these results indicate that a failure in RhoA activation by S1P accounts for the impaired upregulation of motility and endocytosis of *Swap-70*$^{-/-}$ BMDCs.

In vitro transwell assays showed that *Swap-70*$^{-/-}$ BMDCs migrate poorly to S1P. Video microscopic analyses of *Swap-70*$^{-/-}$ BMDCs revealed a significant decrease in migratory speed, but not in directionality, when compared with wt BMDCs in response to S1P. This indicates two different mechanisms controlling speed and directionality toward S1P, and that SWAP-70 regulates the former. In addition, this indicates that functional S1P receptors are expressed and locate on the surface of *Swap-70*$^{-/-}$ BMDCs, in agreement with their wt-like expression levels of S1PR mRNA and proteins. Interestingly, wt and *Swap-70*$^{-/-}$ BMDCs showed no difference in in vitro migration to CCL19 and CCL21. S1P and chemokines signal through GPCRs, which activate Rho GTPases necessary for the cytoskeletal rearrangements involved in migration of cells (10, 47). In DCs, signaling through CCR7 also activates RhoA, but this modulates only the migratory speed and not CCR7-dependent chemotaxis (43). We confirmed that inhibition of RhoA activation with exoenzyme C3 does not block CCR7-chemotaxis of BMDCs. In addition, *Swap-70*$^{-/-}$ BMDCs show no difference in migratory speed in response to CCL19 (data not shown) and behave like wt in transwell assays. Consistent with the previous notion (4) that RhoA activation by S1P or by chemokines are independent processes, we conclude that SWAP-70 plays a particular role in RhoA-dependent S1P signaling necessary for DC motility. We found that skin-derived DCs in ears of *Swap-70*$^{-/-}$ mice migrate poorly into dermal lymphatic vessels. *Swap-70*$^{-/-}$ BMDCs showed impaired transmigration through endothelial lymphatic cells in vitro in response to CCL19, which may account for the defect in entering to lymphatic vessels. However, this phenotype may also be caused by failure to activate RhoA and to localize Rac1 and RhoA to centers of actin polymerization after S1P stimulus because $S1P_1$ controls migration of skin-derived DCs to draining lymph nodes (8). Therefore, SWAP-70 may control S1P-dependent signaling and transmigration in skin-derived DCs, two processes that regulate DC migration to lymph nodes (8, 31, 32), an aspect that will be the subject of future studies.

Our previous studies showed interaction of RhoA and SWAP-70 in BMDC lysates, and that RhoA is already activated before arrival of an LPS stimulus in *Swap-70*$^{-/-}$ BMDCs, which suggests the control of RhoA activation by SWAP-70 (14). The abrogation of the preactivated state of RhoA in *Swap-70*$^{-/-}$ BMDCs by treatment with exoenzyme C3 before, but not during, a LPS stimulus restored upregulation of MHC-II on the surface of *Swap-70*$^{-/-}$ BMDCs (14). In this study, we detected a significant difference in the activation state of RhoA in LPS-matured wt and *Swap-70*$^{-/-}$ BMDCs before appearance of the S1P stimulus. Similar to the upregulation of MHC-II in *Swap-70*$^{-/-}$ BMDCs (14), treatment with the exoenzyme C3 before, but not during, the S1P stimulus restored migration to S1P and S1P-induced upregulation of endocytosis in *Swap-70*$^{-/-}$ BMDCs. Pretreatment with C3 also restored proper caveolin and G protein distribution to raft fractions. MHC-II is redistributed to the raft fraction only if the cells were not activated with LPS as described before (14). This indicates that SWAP-70 allows regulated and timely activation of RhoA, and thereby supports a proper response to S1P. SWAP-70 thus constitutes a novel element controlling S1P signaling in DCs.

Morphological analysis of BMDCs moving through pores in a 3D environment in response to S1P showed that wt cells have a rounded body shape and short dendrites that usually point to the direction of cell movement. In contrast, *Swap-70*$^{-/-}$ BMDCs showed an elongated morphology and long dendrites that pointed to different directions at the same time. The nucleus was often lagging behind the cell body. The analysis of *Swap-70*$^{-/-}$ BMDCs without S1P stimulus showed no morphological difference when

Downloaded from http://www.jimmunol.org/ by guest on February 24, 2022

compared with wt cells (data not shown). DC movement in 3D environments is regulated by dynamic actin polymerization at the cell front and actomyosin contractions of the trailing edge to push the nucleus through narrow spaces (17). *Swap-70*$^{-/-}$ BMDCs required more time to move through the pores of the collagen matrix, and as a result, their dendrites are longer and the nucleus was often dragged behind. As a consequence, *Swap-70*$^{-/-}$ BMDCs may fail to retract the trailing edge on time. These observations are in agreement with the failure of *Swap-70*$^{-/-}$ BMDCs to activate RhoA on S1P stimulation, because this Rho GTPase is required for the contraction of the trailing edge of mature DCs moving in collagen matrix (17).

The inhibition of Rac1 through activation of RhoA impairs migration toward S1P in cells expressing only the $S1P_2$ receptor (48, 49). We deem it unlikely that the deficiency of *Swap-70*$^{-/-}$ BMDCs to migrate toward S1P results from deficient S1P signaling through $S1P_2$, because activation of Rac1 on S1P treatment is not significantly different between *Swap-70*$^{-/-}$ and wt BMDCs. However, localization of Rac1 to areas of actin polymerization after S1P stimulus is impaired in *Swap-70*$^{-/-}$ BMDCs. This failure may negatively affect $S1P_1$ signaling. In studies done with different cell lines, it has been concluded that $S1P_1$ only activates Rac1 by $G\alpha_i$ association, whereas $S1P_3$ activates both Rac1 and RhoA by coupling to $G\alpha_i$ and $G\alpha_{12/13}$, respectively (10). In BMDCs lysates, SWAP-70 interacts with Rac1, RhoA (14), and $G\alpha_I$ (this study). It is plausible to hypothesize that SWAP-70 acts at the level of interaction of G proteins with Rho GTPases during S1P signaling and, therefore, that its absence causes poor S1P-induced migration and endocytosis. At which level SWAP-70 regulates other G protein-dependent responses, for example, to chemokines, will be further studied. Both $G\alpha_{12}$ and $G\alpha_{13}$ localize to plasma membrane (50), and their compartmentalization into membrane rafts/caveolae can provide rapid and strong activation signaling (51, 52). In both immature wt and *Swap-70*$^{-/-}$ BMDCs, a fraction $G\alpha_{13}$, as well as the Rac1 activator $G\alpha_I$, localized into membrane rafts/caveolae. After LPS and S1P stimulus, $G\alpha_{13}$ is absent from membrane rafts/caveolae in *Swap-70*$^{-/-}$ BMDCs. Failure to localize $G\alpha_{13}$ to membrane rafts/caveolae may lead to poor activation of RhoA in LPS-matured *Swap-70*$^{-/-}$ BMDCs after S1P stimulus. In agreement with this, it has been demonstrated that membrane localization of $G\alpha_{13}$ is necessary to recruit p115-RhoGEF to the membrane for subsequent RhoA activation (53, 54). $G\alpha_I$ was observed to disappear from membrane rafts/caveolae in lysates from both wt and *Swap-70*$^{-/-}$ BMDCs after stimulation with LPS and S1P. This observation is reminiscent of the situation in smooth muscle cells where $G\alpha_I$ and $G\alpha_q$ redistribute to the cytosol after an agonist stimulus (55). This also suggests a mechanism of Rac1 activation different from that of RhoA.

Collectively, our results suggest that SWAP-70 contributes to proper, timely, and stable activation of RhoA in S1P signaling affecting motility and endocytosis in DCs. In addition, given that SWAP-70 interacts with $G\alpha_I$ and $G\alpha_{13}$, and that initial signaling through $G\alpha_{13}$ proteins may be negatively affected by a failure to localize in membrane rafts/caveolae, SWAP-70 is of considerable biological significance in S1P-induced functions of mature DCs.

Disclosures

The authors have no financial conflicts of interest.

References

1. Banchereau, J., F. Briere, C. Caux, J. Davoust, S. Lebecque, Y. J. Liu, B. Pulendran, and K. Palucka. 2000. Immunobiology of dendritic cells. *Annu. Rev. Immunol.* 18: 767–811.
2. Rosen, H., and E. J. Goetzl. 2005. Sphingosine 1-phosphate and its receptors: an autocrine and paracrine network. *Nat. Rev. Immunol.* 5: 560–570.
3. Pappu, R., S. R. Schwab, I. Cornelissen, J. P. Pereira, J. B. Regard, Y. Xu, E. Camerer, Y. W. Zheng, Y. Huang, J. G. Cyster, and S. R. Coughlin. 2007. Promotion of lymphocyte egress into blood and lymph by distinct sources of sphingosine-1-phosphate. *Science* 316: 295–298.
4. Czeloth, N., G. Bernhardt, F. Hofmann, H. Genth, and R. Förster. 2005. Sphingosine-1-phosphate mediates migration of mature dendritic cells. *J. Immunol.* 175: 2960–2967.
5. Gollmann, G., H. Neuwirt, C. H. Tripp, H. Mueller, G. Konwalinka, C. Heufler, N. Romani, and M. Tiefenthaler. 2008. Sphingosine-1-phosphate receptor type-1 agonism impairs blood dendritic cell chemotaxis and skin dendritic cell migration to lymph nodes under inflammatory conditions. *Int. Immunol.* 20: 911–923.
6. Idzko, M., H. Hammad, M. van Nimwegen, M. Kool, T. Müller, T. Soullié, M. A. Willart, D. Hijdra, H. C. Hoogsteden, and B. N. Lambrecht. 2006. Local application of FTY720 to the lung abrogates experimental asthma by altering dendritic cell function. *J. Clin. Invest.* 116: 2935–2944.
7. Alvarez, D., E. H. Vollmann, and U. H. von Andrian. 2008. Mechanisms and consequences of dendritic cell migration. *Immunity* 29: 325–342.
8. Rathinasamy, A., N. Czeloth, O. Pabst, R. Förster, and G. Bernhardt. 2010. The origin and maturity of dendritic cells determine the pattern of sphingosine 1-phosphate receptors expressed and required for efficient migration. *J. Immunol.* 185: 4072–4081.
9. Sanchez, T., and T. Hla. 2004. Structural and functional characteristics of S1P receptors. *J. Cell. Biochem.* 92: 913–922.
10. Taha, T. A., K. M. Argraves, and L. M. Obeid. 2004. Sphingosine-1-phosphate receptors: receptor specificity versus functional redundancy. *Biochim. Biophys. Acta* 1682: 48–55.
11. Maeda, Y., H. Matsuyuki, K. Shimano, H. Kataoka, K. Sugahara, and K. Chiba. 2007. Migration of CD4 T cells and dendritic cells toward sphingosine 1-phosphate (S1P) is mediated by different receptor subtypes: S1P regulates the functions of murine mature dendritic cells via S1P receptor type 3. *J. Immunol.* 178: 3437–3446.
12. Radeke, H. H., H. von Wenckstern, K. Stoidtner, B. Sauer, S. Hammer, and B. Kleuser. 2005. Overlapping signaling pathways of sphingosine 1-phosphate and TGF-beta in the murine Langerhans cell line XS52. *J. Immunol.* 174: 2778–2786.
13. Oberbanscheidt, P., S. Balkow, J. Kühnl, S. Grabbe, and M. Bähler. 2007. SWAP-70 associates transiently with macropinosomes. *Eur. J. Cell Biol.* 86: 13–24.
14. Ocana-Morgner, C., C. Wahren, and R. Jessberger. 2009. SWAP-70 regulates RhoA/RhoB-dependent MHCII surface localization in dendritic cells. *Blood* 113: 1474–1482.
15. Burns, S., S. J. Hardy, J. Buddle, K. L. Yong, G. E. Jones, and A. J. Thrasher. 2004. Maturation of DC is associated with changes in motile characteristics and adherence. *Cell Motil. Cytoskeleton* 57: 118–132.
16. Burns, S., A. J. Thrasher, M. P. Blundell, L. Machesky, and G. E. Jones. 2001. Configuration of human dendritic cell cytoskeleton by Rho GTPases, the WAS protein, and differentiation. *Blood* 98: 1142–1149.
17. Lämmermann, T., B. L. Bader, S. J. Monkley, T. Worbs, R. Wedlich-Söldner, K. Hirsch, M. Keller, R. Förster, D. R. Critchley, R. Fässler, and M. Sixt. 2008. Rapid leukocyte migration by integrin-independent flowing and squeezing. *Nature* 453: 51–55.
18. Lämmermann, T., J. Renkawitz, X. Wu, K. Hirsch, C. Brakebusch, and M. Sixt. 2009. Cdc42-dependent leading edge coordination is essential for interstitial dendritic cell migration. *Blood* 113: 5703–5710.
19. Quast, T., B. Tappertzhofen, C. Schild, J. Grell, N. Czeloth, R. Förster, R. Alon, L. Fraemohs, K. Dreck, C. Weber, et al. 2009. Cytohesin-1 controls the activation of RhoA and modulates integrin-dependent adhesion and migration of dendritic cells. *Blood* 113: 5801–5810.
20. Wang, Z., Y. Kumamoto, P. Wang, X. Gan, D. Lehmann, A. V. Smrcka, L. Cohn, A. Iwasaki, L. Li, and D. Wu. 2009. Regulation of immature dendritic cell migration by RhoA guanine nucleotide exchange factor Arhgef5. *J. Biol. Chem.* 284: 28599–28606.
21. Ihara, S., T. Oka, and Y. Fukui. 2006. Direct binding of SWAP-70 to non-muscle actin is required for membrane ruffling. *J. Cell Sci.* 119: 500–507.
22. Shinohara, M., Y. Terada, A. Iwamatsu, A. Shinohara, N. Mochizuki, M. Higuchi, Y. Gotoh, S. Ihara, S. Nagata, H. Itoh, et al. 2002. SWAP-70 is a guanine-nucleotide-exchange factor that mediates signalling of membrane ruffling. *Nature* 416: 759–763.
23. Matloubian, M., C. G. Lo, G. Cinamon, M. J. Lesneski, Y. Xu, V. Brinkmann, M. L. Allende, R. L. Proia, and J. G. Cyster. 2004. Lymphocyte egress from thymus and peripheral lymphoid organs is dependent on S1P receptor 1. *Nature* 427: 355–360.
24. Gunzer, M., A. Schäfer, S. Borgmann, S. Grabbe, K. S. Zänker, E. B. Bröcker, E. Kämpgen, and P. Friedl. 2000. Antigen presentation in extracellular matrix: interactions of T cells with dendritic cells are dynamic, short lived, and sequential. *Immunity* 13: 323–332.
25. Tripp, C. H., B. Haid, V. Flacher, M. Sixt, H. Peter, J. Farkas, R. Gschwentner, L. Sorokin, N. Romani, and P. Stoitzner. 2008. The lymph vessel network in mouse skin visualised with antibodies against the hyaluronan receptor LYVE-1. *Immunobiology* 213: 715–728.
26. Lingwood, D., and K. Simons. 2007. Detergent resistance as a tool in membrane research. *Nat. Protoc.* 2: 2159–2165.
27. Bowles, R., S. Patil, H. Pincas, and S. C. Sealfon. 2010. Validation of efficient high-throughput plasmid and siRNA transfection of human monocyte-derived dendritic cells without cell maturation. *J. Immunol. Methods* 363: 21–28.

Downloaded from http://www.jimmunol.org/ by guest on February 24, 2022

28. Pham, T. H., P. Baluk, Y. Xu, I. Grigorova, A. J. Bankovich, R. Pappu, S. R. Coughlin, D. M. McDonald, S. R. Schwab, and J. G. Cyster. 2010. Lymphatic endothelial cell sphingosine kinase activity is required for lymphocyte egress and lymphatic patterning. *J. Exp. Med.* 207: 17–27.
29. Kissenpfennig, A., S. Henri, B. Dubois, C. Laplace-Builhé, P. Perrin, N. Romani, C. H. Tripp, P. Douillard, L. Leserman, D. Kaiserlian, et al. 2005. Dynamics and function of Langerhans cells in vivo: dermal dendritic cells colonize lymph node areas distinct from slower migrating Langerhans cells. *Immunity* 22: 643–654.
30. Shklovskaya, E., B. Roediger, and B. Fazekas de St Groth. 2008. Epidermal and dermal dendritic cells display differential activation and migratory behavior while sharing the ability to stimulate CD4+ T cell proliferation in vivo. *J. Immunol.* 181: 418–430.
31. Johnson, L. A., S. Clasper, A. P. Holt, P. F. Lalor, D. Baban, and D. G. Jackson. 2006. An inflammation-induced mechanism for leukocyte transmigration across lymphatic vessel endothelium. *J. Exp. Med.* 203: 2763–2777.
32. Johnson, L. A., and D. G. Jackson. 2010. Inflammation-induced secretion of CCL21 in lymphatic endothelium is a key regulator of integrin-mediated dendritic cell transmigration. *Int. Immunol.* 22: 839–849.
33. Ledgerwood, L. G., G. Lal, N. Zhang, A. Garin, S. J. Esses, F. Ginhoux, M. Merad, H. Peche, S. A. Lira, Y. Ding, et al. 2008. The sphingosine 1-phosphate receptor 1 causes tissue retention by inhibiting the entry of peripheral tissue T lymphocytes into afferent lymphatics. *Nat. Immunol.* 9: 42–53.
34. Pearce, G., V. Angeli, G. J. Randolph, T. Junt, U. von Andrian, H. J. Schnittler, and R. Jessberger. 2006. Signaling protein SWAP-70 is required for efficient B cell homing to lymphoid organs. *Nat. Immunol.* 7: 827–834.
35. Randolph, G. J., V. Angeli, and M. A. Swartz. 2005. Dendritic-cell trafficking to lymph nodes through lymphatic vessels. *Nat. Rev. Immunol.* 5: 617–628.
36. Yanagawa, Y., and K. Onoé. 2003. CCR7 ligands induce rapid endocytosis in mature dendritic cells with concomitant up-regulation of Cdc42 and Rac activities. *Blood* 101: 4923–4929.
37. Fernandez-Borja, M., L. Janssen, D. Verwoerd, P. Hordijk, and J. Neefjes. 2005. RhoB regulates endosome transport by promoting actin assembly on endosomal membranes through Dia1. *J. Cell Sci.* 118: 2661–2670.
38. Wallar, B. J., A. D. Deward, J. H. Resau, and A. S. Alberts. 2007. RhoB and the mammalian Diaphanous-related formin mDia2 in endosome trafficking. *Exp. Cell Res.* 313: 560–571.
39. Morandat, S., and K. El Kirat. 2007. Solubilization of supported lipid membranes by octyl glucoside observed by time-lapse atomic force microscopy. *Colloids Surf. B Biointerfaces* 55: 179–184.
40. Insel, P. A., B. P. Head, H. H. Patel, D. M. Roth, R. A. Bundey, and J. S. Swaney. 2005. Compartmentation of G-protein-coupled receptors and their signalling components in lipid rafts and caveolae. *Biochem. Soc. Trans.* 33: 1131–1134.
41. Patel, H. H., F. Murray, and P. A. Insel. 2008. Caveolae as organizers of pharmacologically relevant signal transduction molecules. *Annu. Rev. Pharmacol. Toxicol.* 48: 359–391.
42. Aktories, K., C. Wilde, and M. Vogelsgesang. 2004. Rho-modifying C3-like ADP-ribosyltransferases. *Rev. Physiol. Biochem. Pharmacol.* 152: 1–22.
43. Riol-Blanco, L., N. Sánchez-Sánchez, A. Torres, A. Tejedor, S. Narumiya, A. L. Corbí, P. Sánchez-Mateos, and J. L. Rodríguez-Fernández. 2005. The chemokine receptor CCR7 activates in dendritic cells two signaling modules that independently regulate chemotaxis and migratory speed. *J. Immunol.* 174: 4070–4080.
44. Raftopoulou, M., and A. Hall. 2004. Cell migration: Rho GTPases lead the way. *Dev. Biol.* 265: 23–32.
45. Albiges-Rizo, C., O. Destaing, B. Fourcade, E. Planus, and M. R. Block. 2009. Actin machinery and mechanosensitivity in invadopodia, podosomes and focal adhesions. *J. Cell Sci.* 122: 3037–3049.
46. Berdeaux, R. L., B. Díaz, L. Kim, and G. S. Martin. 2004. Active Rho is localized to podosomes induced by oncogenic Src and is required for their assembly and function. *J. Cell Biol.* 166: 317–323.
47. Thelen, M. 2001. Dancing to the tune of chemokines. *Nat. Immunol.* 2: 129–134.
48. Okamoto, H., N. Takuwa, T. Yokomizo, N. Sugimoto, S. Sakurada, H. Shigematsu, and Y. Takuwa. 2000. Inhibitory regulation of Rac activation, membrane ruffling, and cell migration by the G protein-coupled sphingosine-1-phosphate receptor EDG5 but not EDG1 or EDG3. *Mol. Cell. Biol.* 20: 9247–9261.
49. Sugimoto, N., N. Takuwa, H. Okamoto, S. Sakurada, and Y. Takuwa. 2003. Inhibitory and stimulatory regulation of Rac and cell motility by the G12/13-Rho and Gi pathways integrated downstream of a single G protein-coupled sphingosine-1-phosphate receptor isoform. *Mol. Cell. Biol.* 23: 1534–1545.
50. Veit, M., B. Nürnberg, K. Spicher, C. Harteneck, E. Ponimaskin, G. Schultz, and M. F. Schmidt. 1994. The alpha-subunits of G-proteins G12 and G13 are palmitoylated, but not amidically myristoylated. *FEBS Lett.* 339: 160–164.
51. Bhatnagar, A., D. J. Sheffler, W. K. Kroeze, B. Compton-Toth, and B. L. Roth. 2004. Caveolin-1 interacts with 5-HT2A serotonin receptors and profoundly modulates the signaling of selected Galphaq-coupled protein receptors. *J. Biol. Chem.* 279: 34614–34623.
52. Oh, P., and J. E. Schnitzer. 2001. Segregation of heterotrimeric G proteins in cell surface microdomains. G(q) binds caveolin to concentrate in caveolae, whereas G(i) and G(s) target lipid rafts by default. *Mol. Biol. Cell* 12: 685–698.
53. Bhattacharyya, R., J. Banerjee, K. Khalili, and P. B. Wedegaertner. 2009. Differences in Galpha12- and Galpha13-mediated plasma membrane recruitment of p115-RhoGEF. *Cell. Signal.* 21: 996–1006.
54. Bhattacharyya, R., and P. B. Wedegaertner. 2000. Galpha 13 requires palmitoylation for plasma membrane localization, Rho-dependent signaling, and promotion of p115-RhoGEF membrane binding. *J. Biol. Chem.* 275: 14992–14999.
55. Murthy, K. S., and G. M. Makhlouf. 2000. Heterologous desensitization mediated by G protein-specific binding to caveolin. *J. Biol. Chem.* 275: 30211–30219.

Downloaded from http://www.jimmunol.org/ by guest on February 24, 2022